Journal of the European Ceramic Society **15** (1995) 1221–1228

0955-2219(95)00085-2
0955-2219/95/$9.50

Phase Transformations in Sm (α+β)-SiAlON Ceramics during Post-sintering Heat Treatments

Rupeng Zhao & Yi-Bing Cheng*

Department of Materials Engineering, Monash University, Melbourne 3168, Australia

(Received 14 February 1995; revised version received 19 May 1995; accepted 22 May 1995)

Abstract

Phase transformations in Sm (α + β)-SiAlON ceramics during post-sintering heat treatments at 1300 and 1450°C were investigated using XRD, SEM, TEM and EDS techniques. The transformation from α to β SiAlON, (i.e. α' to β') phases was observed at both temperatures. However, other phase transformations occur simultaneously at grain boundaries of the materials and also involve the β' phase, namely, Glass $\rightarrow$ $SmAlO_3$ + β' and $SmAlO_3$ + $\beta' \rightarrow M'$. Their effects on the amount of β' in the materials must therefore be considered in the study of the α' to β' transformation. It is thought that the increase in the β':(α' + β') ratio during a heat treatment process depends not only on the rate of the α' to β' transformation, but also on the amount and composition of the intergranular phases.

1 Introduction

Post-sintering heat treatment is a technique commonly used in manufacturing SiAlON ceramics. The main objective of the post-sintering heat treatment includes the crystallisation of the glassy grain boundary phase in the materials to improve the materials' performance at elevated temperatures. This is usually achieved via a conventional glass-ceramic process during which the glass devitrifies at a temperature above its T_g point but without being 'melted'.[1,2] There has been much work in understanding of the grain boundary crystallisation, but very little attention has been paid to the effects of the post-sintering heat treatment on the stability of SiAlON phases until very recently. Mandal *et al.*[3] found that some α-SiAlON (α') phases could transform to β-SiAlON (β') during the process. It was observed that the transformation from α' to β' readily occurred in some rare earth α' + β' composite materials when heat-treated between 1000 and 1600°C and the extent of the transformation was more pronounced with increasing temperatures.[3] α' and β' have different mechanical properties,[4] therefore, these findings have opened a new possibility of tailoring the microstructures and properties of SiAlON ceramics in a way that was previously not expected.

α' and β' are two different crystallographic modifications of SiAlON structures.[5] Although both phases are basically built up of corner-sharing (Si,Al)(O, N)$_4$ tetrahedra, there is a distinct difference in the atomic arrangement between the two phases.[6] The bonds in SiAlON structures are strongly covalent and the atoms have a very low self-diffusivity even at 1800°C; these features bear the virtual responsibility of a relatively poor densification behaviour of Si_3N_4-based materials. The transformation between the α' and β' phases has a reconstructive nature which involves the breaking of chemical bonds and substantial atomic diffusion, and hence requires significant amounts of thermal energy. The transformation from α-Si_3N_4 to β-Si_3N_4 did not occur without the presence of a liquid phase in which α-Si_3N_4 grains could dissolve above ~ 1400°C.[7] All these facts naturally raise some questions on the mechanism of α' to β' phase transformations, particularly those taking place at temperatures below the eutectic of the system. The present paper provides some evidence of the α' to β' phase transformation in a Sm α' + β' ceramic composite at both below and above the eutectic temperatures, and further reveals additional phase transformations that could involve the β' phase during post-sintering heat treatments.

2 Experimental Details

Samples were prepared from Si_3N_4 (Starck, Berlin, LC10), AlN (Starck, Berlin, Grade B), Al_2O_3 (Alcoa, A17) and Sm_2O_3 (RE Acton, Rare Earth Products, 99.9%) powders with a starting composition

*To whom correspondence should be addressed.

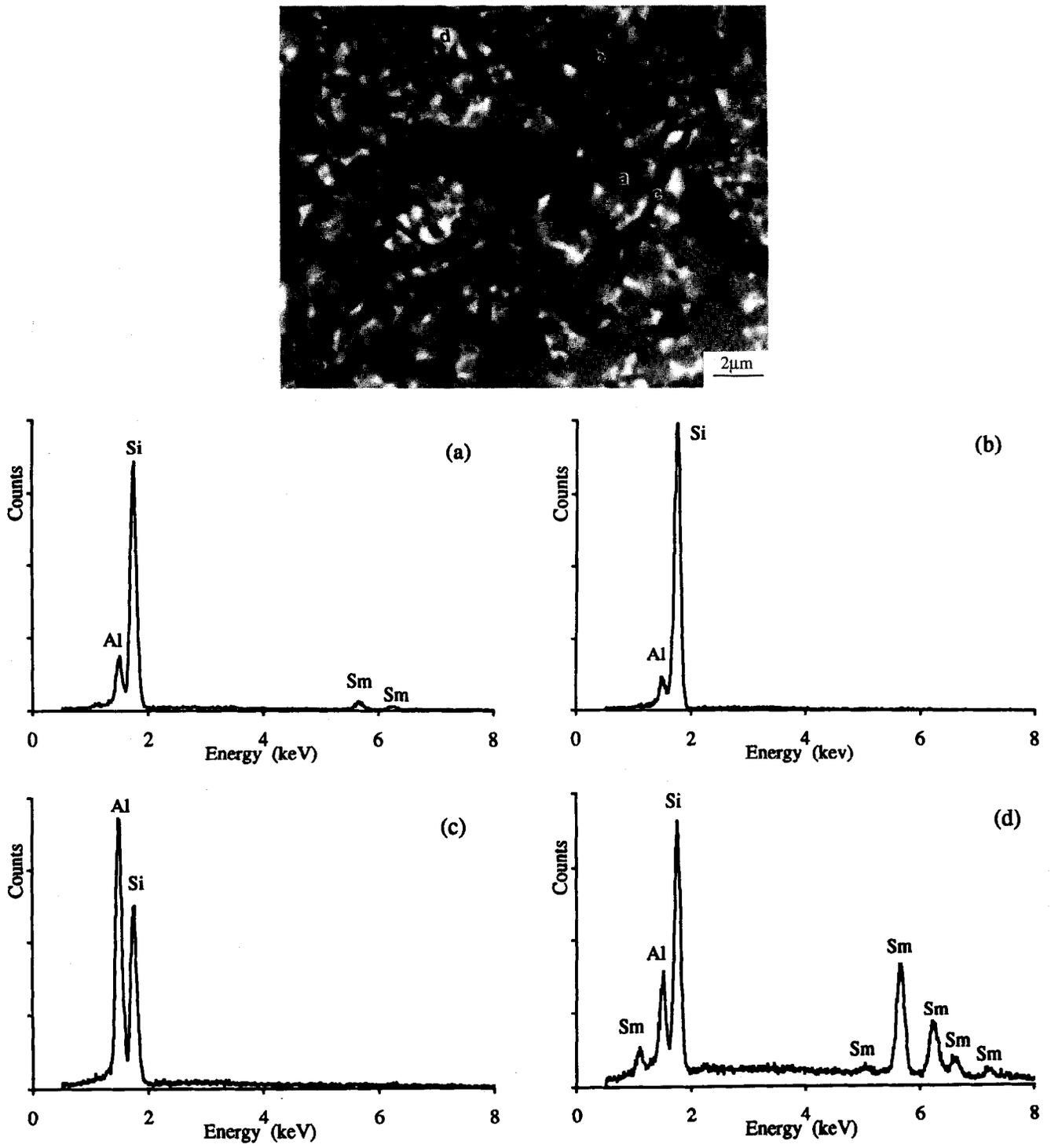

Fig. 1. SEM backscattered image of the as-sintered sample and EDS spectra from different phases. The white regions are intergranular glass, the grey grains are α' and the dark grains either β' or 21R. The EDS spectra of: (a) α'; (b) β'; (c) 21R and (d) grain boundary glass correspond to the regions marked on the micrograph.

of $Sm_{0.379}Si_{9.548}Al_{2.381}O_{1.668}N_{14.403}$. The pelleted green body of the designed composition was initially sintered at 1820°C for 4 h in an industrial furnace. The slow cooling rate of the furnace produced a SiAlON material with wollastonite as the grain boundary phase. Further sintering was carried out in a laboratory carbon resistance furnace at 1800°C for 30 min and the specimen was then cooled in the furnace. Due to a much faster cooling rate, the final material contains mainly α', a small amount of β' and 21R phases with an amorphous phase at grain boundaries.

The samples that contained glassy grain boundaries were subsequently heat-treated at 1300 and 1450°C respectively for various periods. The heat treatments were carried out in flowing nitrogen in an alumina tube furnace with heating and cooling rates of 3°C/min. After heat treatments, the surfaces of the samples were removed by grinding on SiC paper and the bulk of the material was exposed for

crystalline phase and microstructural examinations.

Scanning electron microscopy (SEM) observations and energy-dispersive X-ray spectroscopy analysis (EDS) were carried out using a JEOL 840A instrument. A JAVA image analyser was used to analyse the backscattered SEM electron images. A Philip CM20 TEM instrument fitted with an ultrathin-window EDS detector was used for microstructural observations and compositional analyses. Specimens for TEM were mechanically ground, dimpled to thickness of ~20 μm, and then ion-milled to electron transparency. All specimens were carbon coated before SEM and TEM observations to avoid surface charging.

Phase characterisation was performed with X-ray diffraction (XRD) using a Rigaku X-ray diffractometer. The relative amounts of α' and β' phases, i.e. the β':(α' + β') weight ratio, were calculated using the calibration curves developed by Liddell[8] with the intensities of the (210) peaks of both the α' and β' phases.

$$\beta'(\text{wt\%}) = K/[I_\alpha(210)/I_\beta(210) + K] \times 100\% \quad (1)$$

where K is a constant, equal to 0·702.

The amounts of crystalline grain boundary phases (namely, $SmAlO_3$ and the Al-containing N–melilite, M'[9]) after heat treatments were estimated by comparing appropriate XRD peak intensities of these phases with that of the 21R phase which remained unchanged throughout the heat treatment process. The specific result calculated from this way may possess a certain error, but the trends, i.e. the relative changes in the amount of $SmAlO_3$ and M' phases versus the heat treatment time and temperature, should be indicative. This is true for the β':(α' + β') ratio as well.

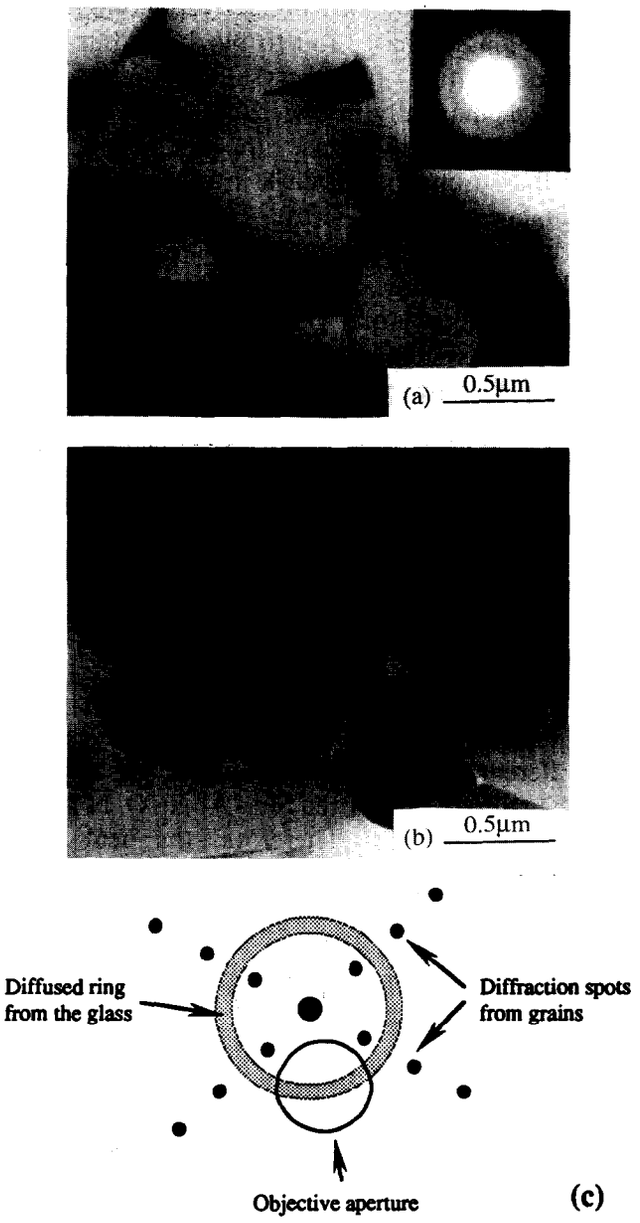

Fig. 2. TEM: (a) bright field and (b) diffused dark field images from the as-sintered specimen. (c) Schematic illustration of the objective aperture position for diffused dark field imaging. The glassy nature of the grain boundary phase is indicated by the electron diffraction rings (inset in (a)).

3 Results

3.1 The as-sintered materials

XRD analyses showed that the crystalline phases in the as-sintered sample consisted of mainly α' and β' phases, with a small amount of 21R polytypoid phase. The β':(α' + β') ratio was about 11%. Figure 1 shows a typical SEM backscattered image of the as-sintered material. Since the backscattered electron intensity depends mainly on the mean atomic number, the differences in the amounts of samarium presented in the α', β' and grain boundary phases make them easily identified. The white grain boundary regions are the intergranular glassy phase containing large amounts of samarium. The equiaxed grey regions are α' grains with a small amount of samarium, and the dark regions are β' or 21R phases with no samarium. This has been supported by the EDS analytical results (Fig. 1). The β' and 21R phases can be differentiated by EDS analyses or by their morphology. The needle-like grains with high aspect ratios are usually the 21R phase while the slightly elongated ones with low aspect ratios are β'. Image analyses indicate that the as-sintered sample contained around 75% α' and 10% intergranular glassy phase, with the rest being β' and 21R.

Figure 2 shows typical bright field and diffused dark field TEM images of the as-sintered sample. In the bright field image, the intergranular phase is darker because of its high samarium content. Diffused dark field images are obtained by using the objective aperture of the microscope to select

a part of the diffraction ring corresponding to the expected glassy phase, and to block all diffraction spots originating from crystalline grains,[10] as shown schematically in Fig. 2(c). As a result, the intergranular glassy phase appears bright while crystalline grains are all dark in the diffused dark field image (see Fig. 2(b)). Electron diffraction confirmed that the intergranular phase was amorphous, as indicated by the ring pattern (Fig. 2(a)). The intergranular glass comprises all five elements in the system, although its composition may vary slightly from pockets to pockets (Fig. 3). To a first order approximation (using calculated parameters and neglecting absorption effect), the estimated composition of the glass is around Sm:Si:Al = 0·7:1·0:0·8 and N:O = 1:2·3 (in atomic ratio). Therefore, the Si, O and N contents in the glass are significant.

3.2 Heat treatment at 1300°C

Post-sintering heat treatment was conducted at both 1300 and 1450°C respectively to investigate the different phase transformation behaviour. The eutectic temperature of the Sm– Al–Si–O–N system is about 1350°C.[11,12] Therefore, the heat treatments at 1300 and 1450°C represents the thermal processes below and above the eutectic temperature of the system respectively.

Samarium aluminate ($SmAlO_3$) was observed as the only devitrification product of the intergranular glass in the sample heat-treated at 1300°C. XRD results of the samples after heat treatments at this temperature for various periods are presented in Fig. 4. Both the β':(α' + β') ratio and the amount of $SmAlO_3$ increased with the duration of the heat treatment. The increases in $SmAlO_3$ and the β':(α' + β') ratio can be divided into two distinct stages according to the rate of the phase transformations. There is a rapid increase in both

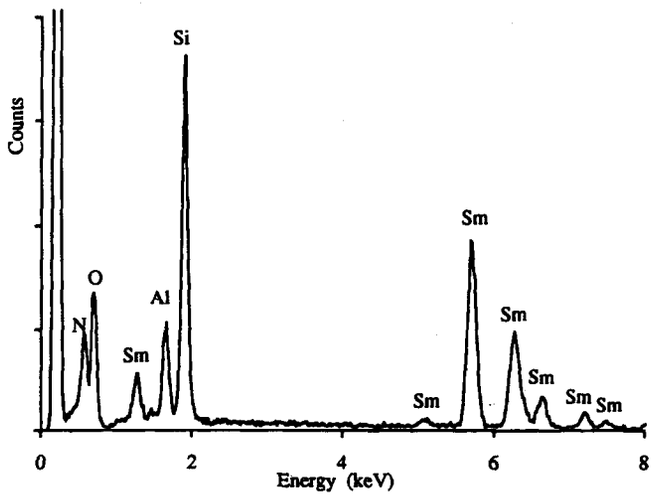

Fig. 3. EDS spectrum from the intergranular glassy phase in the material showing that it contains significant amounts of Si and N.

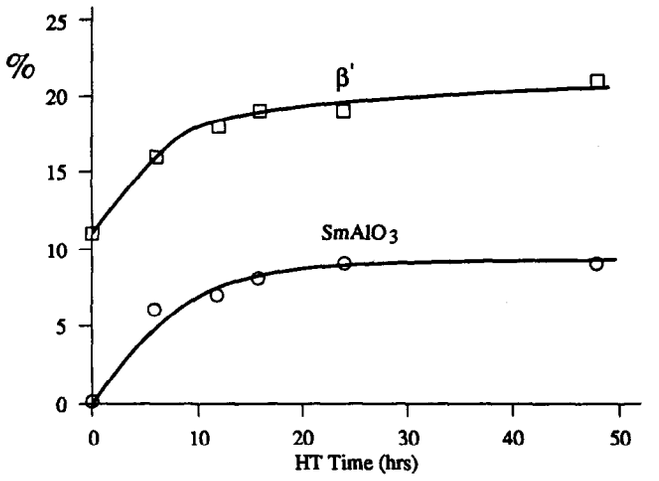

Fig. 4. The β':(α' + β') ratio and the relative $SmAlO_3$ fraction of the samples heat-treated at 1300°C as a function of heat treatment time.

$SmAlO_3$ and β' phases in the initial heat treatment stage ($0 < t < 6$ h). Further heat treatment up to 48 h resulted in only a slight increase in these two phases. The initial rapid increase in $SmAlO_3$ indicates that the intergranular glassy phase devitrifies very rapidly at the temperature, and grain boundary

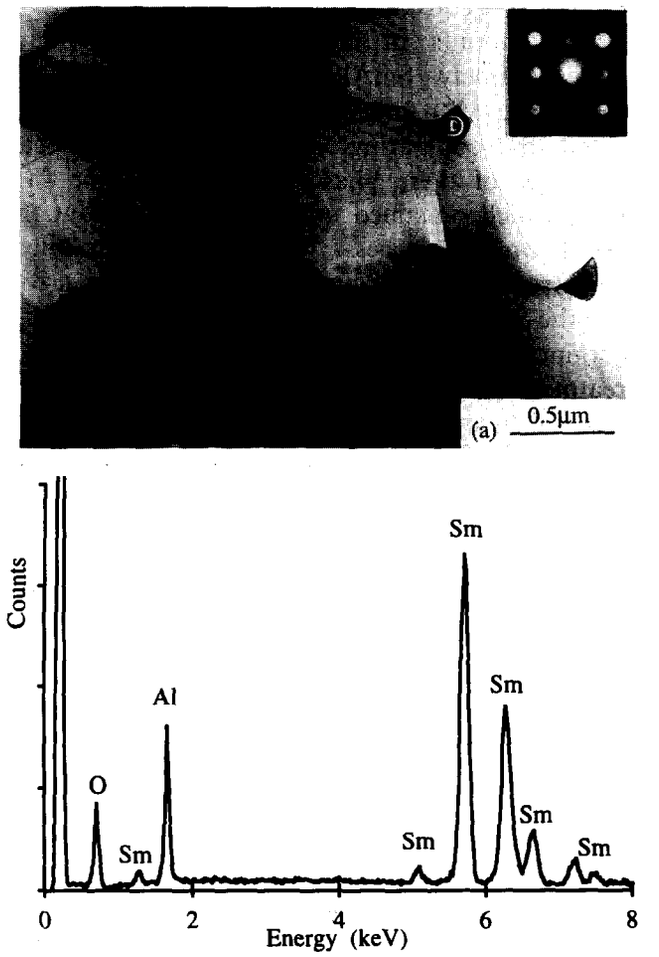

Fig. 5. (a) Typical TEM bright field image of the sample heat-treated at 1300°C for 24 h. The dark crystals at the grain boundaries are $SmAlO_3$ with an orthorhombic structure, as confirmed by electron diffraction from the crystal marked 'D' (inset) and by EDS analysis (b). The diffraction pattern is [001] zone for $SmAlO_3$.

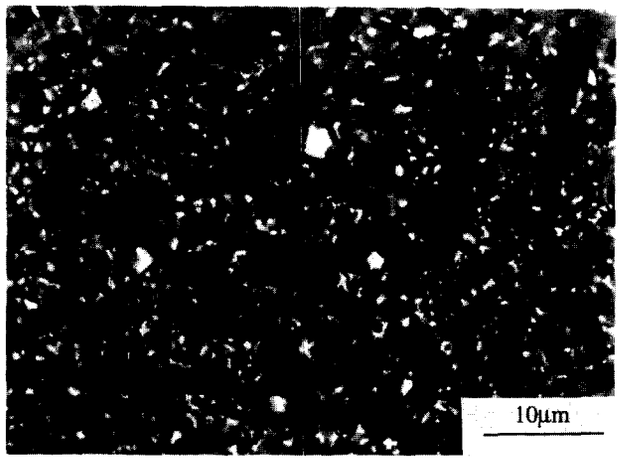

Fig. 6. SEM backscattered image of the sample after heat treatment at 1300°C for 24 h showing homogeneous distribution of $SmAlO_3$ crystals (the white phase).

devitrification may have been completed in a few hours. It is interesting to notice that the increase in the β':(α' + β') ratio follows a similar pattern as that of $SmAlO_3$.

TEM observations revealed that the glass phase in all multiple junctions of the as-received samples was fully crystallised after the heat treatment at 1300°C for 24 h. A typical bright field image is shown in Fig. 5(a). EDS analysis (Fig. 5(b)) and electron diffraction (Fig. 5(a)) confirmed $SmAlO_3$ as the intergranular crystalline phase. SEM observations on all samples heat-treated at 1300°C showed that apart from a few agglomerates of about 2 μm in size, the $SmAlO_3$ grains in general were homogeneously distributed, as shown in Fig. 6, indicating that there was no significant grain boundary migration during the heat treatment at this temperature.

3.3 Heat treatment at 1450°C

Figure 7 summarises the XRD results of the samples after heat treatments at 1450°C for various times. It can be seen from the figure that the β':(α' + β') ratio increases with the duration of the heat treatment. Such an increase in the β' phase can be partially explained in terms of the α' to β' transformation.[3] However, it has been noted that the rate of the increase in β' contents varies significantly with the heat treatment time; as a result, three distinct stages are recognised. In the first few hours, the β':(α' + β') ratio increases rapidly, more than 10% in 4 h. In the second stage (4 h < t < 16 h), the amount of β' remains almost unchanged. With further time, however, the β' phase increases again in the third stage (t > 16 h), but at a lower rate than that in the initial stage. Such a discrete nature of the change in the β':(α' + β') ratio during an isothermal process cannot be simply explained by the α' to β' transformation alone, and other mechanism(s) may also be involved.

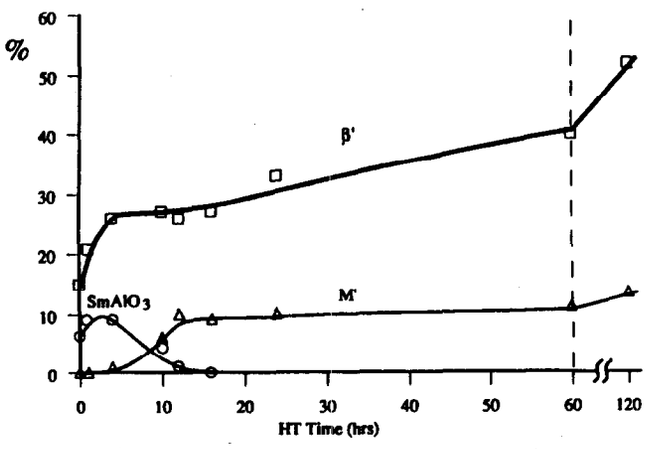

Fig. 7. The β':(α' + β') ratio, $SmAlO_3$ and M' fractions in the samples heat-treated at 1450°C as a function of heat treatment time. The result marked at zero hour in the figure was obtained by heating up the sample to 1450°C and then immediately cooling down to room temperature.

Both $SmAlO_3$ and M' were observed after heat treatment at 1450°C, but their relative contents varied with time. Figure 7 shows the weight fractions of the $SmAlO_3$ and M' phases in the samples. $SmAlO_3$ was observed in the initial stage of the heat treatment at 1450°C prior to the appearance of M'. The amount of $SmAlO_3$ reached a maximum after about 4 h then started to decrease, and completely disappeared after 12 h. The initial heat treatment at 1450°C did not produce any M' phase, but it appeared simultaneously with $SmAlO_3$ after 4 h, and then became the only grain boundary phase at the expense of $SmAlO_3$ in the samples heat-treated for longer than 12 h. There are two interesting correlations among the different phase changes at 1450°C: (i) the initial rapid increase in the β':(α' + β') ratio is associated with the rapid formation of $SmAlO_3$, similar to that observed at 1300°C, suggesting the formation of β' is associated with the devitrification of the intergranular glassy phase; and (ii) the plateau in the curve of the β':(α' + β') ratio is correlated with the decomposition of $SmAlO_3$ and the formation of M'.

Microstructures of the samples heat-treated at 1450°C were studied by SEM. Figures 8(a–c) show three typical SEM backscattered images of the samples heat-treated for 4, 12 and 24 h, respectively. EDS confirmed that the white grain boundary phase in Fig. 8(a) was $SmAlO_3$, while those in Figs 8(b) and (c) were M'. It can be seen from Fig. 8(a) that, as for heat treatment at 1300°C (Fig. 6), most $SmAlO_3$ grains are fine in morphology and are homogeneously distributed at grain boundaries despite a few large agglomerates of around 2 μm. There is virtually little difference in the microstructures of the grain boundary phase between samples heat-treated at 1300°C for 24 h and that at

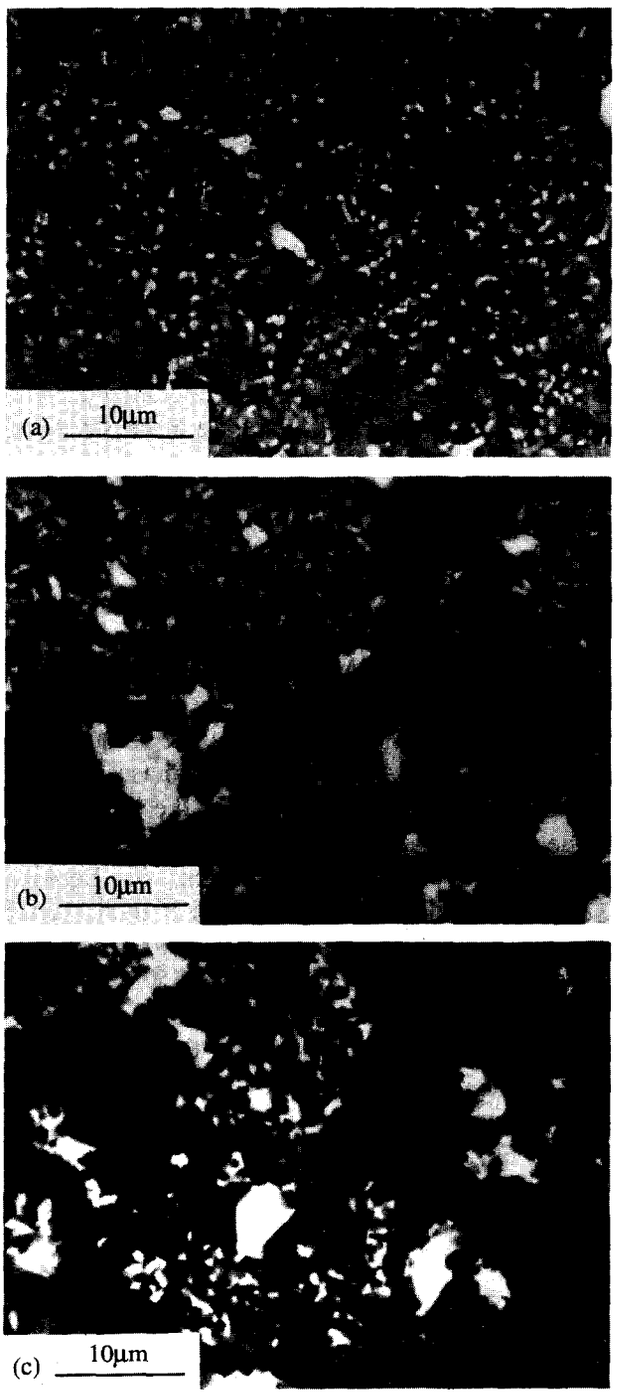

Fig. 8. SEM backscattered images of samples heat-treated at 1450°C for (a) 4 h, (b) 12 h and (c) 24 h. The grain boundary phase (white regions) was $SmAlO_3$ in (a), and the M' phase in both (b) and (c).

1450°C for 4 h, indicating that no significant grain boundary migration occurred when $SmAlO_3$ was formed. As a contrast, the distribution of M' grains is agglomerative and inhomogeneous (Figs 8(b) and (c)), suggesting that considerable intergranular migration has taken place. The grain boundary M' phase forms only above the eutectic temperature,[9] involving a liquid phase which promotes the grain boundary migration. TEM observations on samples heat-treated at 1450°C for 24 h failed to identify any residual amorphous phase (Figs 9 and 10), therefore the liquid phase that

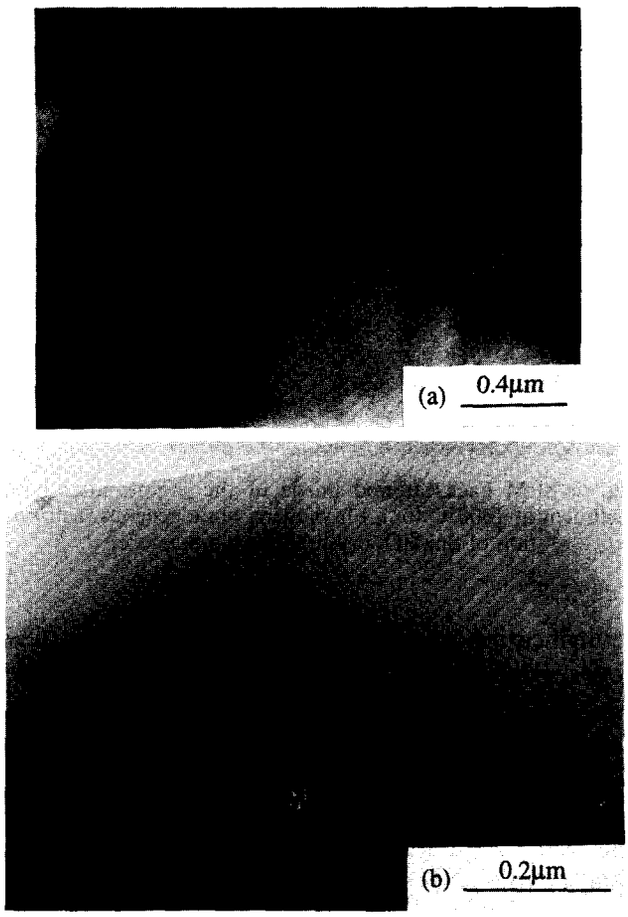

Fig. 9. Typical TEM bright field images of the sample heat-treated at 1450°C for 24 h. Note that little residual glass can be found at grain boundaries. The dark grain in (b) is the M' phase and other grains are either α' or β'.

exists at grain boundaries during the heat treatment must be of a transient nature.

4 Discussion

4.1 β-SiAlON formation during post-sintering heat treatments

The present results have shown that different

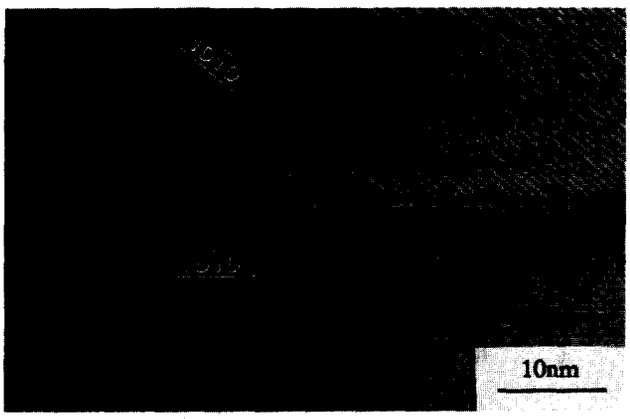

Fig. 10. High resolution lattice fringe image of the boundary between two α' grains in the sample heat-treated at 1450°C for 24 h. Fringes can be followed up to the boundary from either side, indicating the lack of a glass thin film.

phase transformations can take place during post-sintering heat treatments. The increase in the β' concentration after the heat treatments is significant and this provides some evidence for a phase transformation from α' to β' at the heat treatment temperatures. However, due to the simultaneous devitrification of the grain boundary glass and the formation of $SmAlO_3$ and M', other mechanisms may also contribute to the increase in β'.

Although the exact composition of the grain boundary glass is yet to be determined, preliminary EDS analyses indicate that the glassy phase contains all the five elements (Sm–Si–Al–O–N) with significant contents of both Si and N. When $SmAlO_3$ is formed by devitrification, it has consumed most samarium, aluminium and oxygen in the glass, leaving a phase rich in Si and N. However, extensive TEM analyses cannot detect any glassy phase in the samples after devitrification and this leads to a postulation that the residual Si and N in the glass have also formed a crystalline phase in an amount comparable with that of $SmAlO_3$. Considering there is no new unidentified phase from XRD analyses, the anticipated Si and N rich phase formed from the glass must be either α' and/or β'. It is known that Si and N in a glassy phase can partition in the existing SiAlON grains during grain boundary crystallisation.[1] Moreover, the observation of α' to β' transformations in the rare earth SiAlON systems between 1000 and 1500°C[3] indicates a lower free energy for the β' phase than that for the α' phase. Therefore it is thought that the precipitation of β' from the glassy phase is thermodynamically preferred at the present heat-treatment temperatures.

On account of the simultaneous rapid increase in both the β' and $SmAlO_3$ phases in the initial stage of the heat treatment at both 1300 and 1450°C, it is plausible to propose the following phase transformation:

$$\text{Glass} \rightarrow SmAlO_3 + \beta' \qquad (2)$$

Therefore the initial rapid increase in the β':($\alpha' + \beta'$) ratio during the heat treatments is attributed to a combined effect of two different mechanisms, namely, the α' to β' transformation and glass devitrification. The activation energy for the glass devitrification should be much lower than that for the α' to β' transformation at these temperatures, and hence the glass devitrification may make the major contribution to the increase in the β' content at the initial stage of heat treatment processes. The increase in the β':($\alpha' + \beta'$) ratio will therefore depend not only on the heat treatment conditions, but also on the amount and composition of the grain boundary glassy phase in the materials. Significant differences in the extent of the α' to β' phase transformation could occur in samples of the same SiAlON system if the amount and composition of the glassy phase are different.

Table 1. The β': ($\alpha' + \beta'$) ratio of two groups of samples after heat treatment at 1450°C

HT time (h) at 1450°C	*Group I (no glass) (%)*	*Group II (with glass) (%)*
Before HT	19	11
4	27	26
24	34	33

Note: The Group I samples were heat-treated at 1300°C for 24 h and contained $SmAlO_3$ as a grain boundary phase prior to the heat treatment at 1450°C, whereas the Group II samples were as-sintered with a glassy grain boundary phase before the heat treatment.

The proposed mechanism of the transformation, eqn (2), is further supported by another set of experiments in which two groups of samples are compared. Both groups were originally from the same bulk specimen and heat-treated at 1450°C for 4 and 24 h respectively. Prior to this heat treatment, the Group I samples were preheat-treated at 1300°C for 24 h, hence containing $SmAlO_3$ and very little glass, while the Group II samples had no pre-heat treatment and contained a glassy phase at grain boundaries. Table 1 shows the results after the heat treatment at 1450°C. Although the same amount of β' was found in both groups after heat treatments for 4 and 24 h, there appeared a significant difference in the rate of β' increase during the initial 4 h; the sample with a glassy phase (Group II) had a much higher yield of β' compared to the one that contained $SmAlO_3$ prior to the heat treatment (Group I). It is apparent that crystallisation of the intergranular glassy phase has made a significant contribution to the higher increase in the β':($\alpha' + \beta'$) ratio in Group II samples and so this is in agreement with the proposed transformation of eqn (3).

4.2 β-SiAlON consumption during phase transformations

Cheng and Thompson[13] found that the M' phase was the only stable intergranular crystalline phase above 1400°C in the Sm ($\alpha + \beta$)-SiAlON system. Although $SmAlO_3$ was observed in the initial stage of the heat treatment at 1450°C, possibly formed during the slow heating and cooling, it became unstable and formed a eutectic liquid through a reaction with other phases in the system upon further 1450°C heat-treatment. The experimental results indicate that the decomposition of $SmAlO_3$ results in the precipitation of the M'($Sm_3Si_2AlO_4N_3$) phase at the SiAlON grain-boundaries. However, the significant compositional

difference between these two phases implies that the phase transformation must involve an additional Si and N rich phase to complement the Sm–Al–O composition of the grain boundaries. The coincidence between the M' formation and the plateau in the curve of the β':(α' + β') ratio of Fig. 7 suggests that $SmAlO_3$ may have reacted with the β' phase to form a transient liquid necessary for the M' phase precipitation:

$$SmAlO_3 + \beta' \rightarrow \text{liquid} \rightarrow M' \qquad (3)$$

The existence of this transient liquid is supported by the observation that considerable grain boundary migration occurs when the M' phase forms (Fig. 8). The consumption of β' in the above reaction may be compensated by the simultaneous α' to β' transformation. As a result, a balance is maintained and the overall β' content in the sample remains unchanged as shown in Fig. 7. Once reaction (3) is complete, a further steady increase in β' is anticipated.

At 1450°C for 120 h, the relative β' content in the sample was 54%, a significant increase compared to the sample heat-treated for 24 h. This result strongly suggests the transformation from α' to β' during the extended heat treatment. The slight increase in the amount of the M' phase may accommodate the Sm released from the transformed α' structure.

5 Conclusions

Three different phase transformations may occur simultaneously during the post-sintering heat treatment of (α + β)-SiAlON ceramics: (i) grain boundary glass devitrification; (ii) phase transformations among different crystalline grain boundary phases; and (iii) the α' to β' phase transformation. Significant differences in the β':(α' + β') ratio of Sm (α + β)-SiAlON ceramics are observed when the samples are heat-treated at below and above the eutectic temperature of the system. Although there is a transformation between the α' and β' phases during the heat treatments at both the temperatures, other phase transformation mechanisms may also occur and affect the amount of β'.

Devitrification of the intergranular glassy phase can lead to the formation of β' via the transformation

$$\text{Glass} \rightarrow SmAlO_3 + \beta'$$

The amount and composition of the grain boundary glass could have significant effects on the change of the β' phase during the heat treatment. The stabilities of different crystalline intergranular phases may change with temperature, resulting in phase transformations that involve β' phases. In Sm (α + β)-SiAlON materials, the following transformation will take place if the heat treatment is above the eutectic temperature:

$$SmAlO_3 + \beta' \rightarrow \text{liquid} \rightarrow M'$$

These phase transformations may also occur in other rare earth (Ln) (α + β)-SiAlON composites during post-sintering heat-treatments, where the aluminate could be either $LnAlO_3$ or a YAG-type phase. The effects of these transformations on the β':(α' + β') ratio can be significant and have to be taken into account in any studies of the α' to β' phase transformation.

References

1. Lewis, M. H., Crystallisation of grain boundary phases in silicon nitride and SiAlON ceramics. In *Silicon Nitride 93, Key Engineering Materials*, Vol. 89–91, eds M. J. Hoffmann, P. F. Becher & G. Petzow, Trans Tech Publ., 1993 pp. 333–8.
2. Thompson, D. P., New grain boundary phases for nitrogen ceramics. In *MRS Symposium Proceedings: Silicon Nitride Ceramics — Science and Technological Advances*, eds I-Wei Chen *et al.*, MRS, Vol 287, 1993, pp. 79–92.
3. Mandal, H., Thompson, D. P. & Ekström, T., Reversible $\alpha \leftrightarrow \beta$ SiAlON transformation in heat-treated SiAlON ceramics. *J. Eur. Ceram. Soc.*, **12** (1993) 421–9.
4. Ekström, T. & Nygren, M. SiAlON ceramics. *J. Am. Ceram. Soc.*, **75** (1992) 259–76.
5. Jack, K. H., Review: SiAlONS and related nitrogen ceramics. *J. Mater. Sci.*, **11** (1976) 1135–58.
6. Hampshire, S. Nitride ceramics. In *Materials Science and Technology, Vol. 11, Structure and Properties of Ceramics.* ed. M. Swain, VCH, Weinheim, 1994, pp. 121–71.
7. Hampshire, S. & Jack, K. H., The kinetics of densification and phase transformation of nitrogen ceramics. In *Special Ceramics 7, Proc. Brit. Ceram. Soc.*, eds D. W. Taylor and P. Popper, **31** 1981, pp. 37–49.
8. Liddell, K., X-ray analysis of nitrogen ceramic phases, M.Sc Thesis, University of Newcastle upon Tyne, (1979).
9. Cheng, Y.-B. & Thompson, D. P. Aluminium-containing nitrogen melilite phases. *J. Am. Ceram. Soc.*, **77** (1994) 143–8.
10. Clark, D. R., On the detection of thin intergranular films by electron microscopy. *Ultramicroscopy*, **4** (1979) 33–44.
11. Cao, G. Z., Preparation and characterisation of α'-SiAlON ceramics. PhD Thesis, Eindhoven University of Technology (1991).
12. Wang, H. & Yen, T. S., Gas pressure sintering of Re–SiAlON, to be published in J. Eur. Ceram Soc. 1995.
13. Cheng, Y.-B. & Thompson, D. P., Preparation and grain boundary devitrification of samarium α-SiAlON ceramics. *J. Eur. Ceram. Soc.*, **14** (1994) 13–21.